Project information	
Full title:	**REmanufacturing, repurposing and recycling energy goods through advanced Mechatronic and Digital technologies**
Acronym:	R3-Mydas
Grant Agreement number:	101138738 (HORIZON-CL4-2023-TWIN-TRANSITION-01-04 – Innovation Action)

Deliverable

D6.1 – Cognitive robotics & Quality control concept

Dissemination level:	PU - Public, fully open
Type of deliverable:	R - Document, report
Contractual date of delivery:	30 June 2025
Deliverable leader:	CSEM
Status - version, date:	Final – v1.0, 2025-06-26
Keywords:	Cognitive robotics, quality control, remanufacturing

Funded by the European Union

This document is part of a project that is funded by the European Union. Views and opinions expressed are however those of the author(s) only and do not necessarily reflect those of the European Union or the European Health and Digital Executive Agency. Neither the European Union nor the granting authority can be held responsible for them.

Find us at www.r3-mydas.eu.

Executive Summary

The goals of Task 6.1 "Cognitive Robotics" and 6.2 "Quality Control" are to deliver the benefits of robotics and machine learning powered process control to remanufacturing tasks for increased productivity and quality. This is done practically by integrating these frameworks in the implementation of the R3-Mydas demo cases.

By exchanging with the project partners, the demo cases that could benefit most were selected to collaborate.

For Cognitive Robotics, the EV battery recycling demo case of Work Package 3 was selected for implementation of a robotically automated disassembly setup that could save tedious labour hours and increase safety in the processing plant. A concept combining perception, reasoning and execution was designed. The robot should perceive the screws to be disassembled with a computer vision model, reason on what specific task to do next and execute the disassembly thanks to the electric screwdriver fixed at the end-effector. The implementation of this concept has been successful but shows limitations in the identification of screw positions. This problem will be resolved via the implementation of an adaptive framework that refines its guess of the object's position as it approaches it.

Regarding Quality Control, the Crankshaft demo case of Work Package 2 was best suited to benefit from process control. A simulation of the thermal field created by the laser-cladding process was programmed for the purpose of stabilizing the process by adapting the process parameters. By using a fast and generalizable neural operator surrogate, the simulation can run in real-time in order to perform real-time control. The simulation was so far implemented in 2D and will be extrapolated in 3D before being coupled with a Model Prediction Controller that will use its predictions to update the laser-cladding parameters.

These 2cases show how robotics and machine learning can bring value for remanufacturing tasks that often show challenges, in particular because of the uniqueness of each part to be processed.

Deliverable leader:	Johan Poccard
Contributors:	Johan Poccard, Lukas Brock
Reviewers:	Thomas Sølund, Fenia Giannakopoulou
Approved by:	Athanasios Poulakidas, Irene Diamantopoulou (NCI)

Document History			
Version	**Date**	**Contributor(s)**	**Description**
0.1	2025-06-12	Johan Poccard	Creation of document, first draft
0.2	2025-06-18	Johan Poccard	First draft finalized
0.3	2025-06-18	Fenia Giannakopoulou, Thomas Sølund	Review
0.4	2025-06-23	Johan Poccard	Final version before QA
1.0	2025-06-26	Athanasios Poulakidas	Version to be submitted after final QA

Table of Contents

Table of Figures

List of Tables

Definitions, Acronyms and Abbreviations

Acronym/ Abbreviation	Title
AM	Additive Manufacturing
CNO	Convolutional Neural Operator
DED	Direct Energy Deposition
FNO	Fourier Neural Operator
GNN	Graph Neural Network
L-PBF	Laser Power Bed Fusion
LSTM	Long Short-Term Memory
ML	Machine Learning
NO	Neural Operator
PDE	Partial Differential Equation

1 Introduction

1.1 Project Information

Despite the multiple advantages of products remanufacturing, being widely recognised as an effective means for transitioning to a more circular economy, there is still need for improved research and experimental observations, to improve traceability and reliability of the final products from end-users' perspectives, as well as enhanced impacts monitoring. The primary R3-Mydas objective is to develop a multi-actor framework, integrating innovative digital technologies (ML for process and quality control, marketplace, graph models for defects detection, digital twins), advanced mechatronics (AM, laser-cladding, automated disassembly/reassembly) and newly developed approaches from SSH (extended TAM/UTAUT models, ethics and legal framework), for functionally, environmentally and economically sustainable circular value chains for remanufacturing of energy goods at the factory level (Oil & Gas crankshafts – demo 1, E-vehicles batteries – demo 2, Wind turbines gearboxes – demo 3).

R3-Mydas will deliver unprecedented impacts throughout the targeted value chains, as follows: up to 60% time reduction in programming for remanufacturing; up to 20% increased product quality; up to 30% rework reduction [Demo 1]; up to 30% improved detection of tiny deviations from normal behaviour; up to 50% faster anomaly localization; up to 30% increase the number of different modality data streams handled; up to 20% faster fusion process [Demo 2]; up to 99% reusage rate; -90% prevention rate; -75% lead time; up to 85% raw material savings potential [Demo 3]. R3-Mydas will deliver a marketplace associating to each remanufactured product or services/component for remanufacturing a Digital Passport-like set of information, ensuring full traceability. Finally, a dedicated training programme will be designed and delivered by EITM, targeting the P R3-Mydas project remanufacturing value chains (100+ training hours and 100+ diverse stakeholders engaged during the Project).

Table 1: The R3-Mydas consortium.

Number[1]	Name	Country	Short name
1(CO)	NETCOMPANY SA	Luxemburg	NCI
2	EUROPEAN FEDERATION FOR WELDING JOINING AND CUTTING	Belgium	EWF
3	EIT MANUFACTURING SOUTH SRL	Italy	EITM
4	FLENDER FINLAND OY	Finland	FLE-FI
4.1(AE)	FLENDER GMBH	Germany	FLE
5	AVL LIST GMBH	Austria	AVL

[1] CO: Coordinator. AE: Affiliated Entity. AP: Associated Partner.

Number[1]	Name	Country	Short name
6	TALLERES MECANICOS COMAS SLU	Spain	TMCOMAS
7	SPIN ROBOTICS IVS	Denmark	SPIN
8	ASOCIATION DE INVESTIGACION METALURGICA DEL NOROESTE	Spain	AIMEN
9	LAPPEENRANNAN-LAHDEN TEKNILLINEN YLIOPISTO LUT	Finland	LUT
10	INFORMATION TECHNOLOGY FOR MARKET LEADERSHIP	Greece	ITML
11	DEEP BLUE SRL	Italy	DBL
12	CHAROKOPEIO PANEPISTIMIO	Greece	HUA
13	IKERLAN S. COOP	Spain	Ikerlan
14	ZIKNES TECHNOLOGY SL	Spain	Ziknes
15 (AP)	CSEM CENTRE SUISSE D'ELECTRONIQUE ET DE MICROTECHNIQUE SA - RECHERCHE ET DEVELOPPEMENT	Switzerland	CSEM

1.2 Document Scope

This document covers the progress achieved in the context of Tasks 6.1 – Cognitive Robotics and 6.2 – Quality Control. It formulates the concept for the technology developed in each task and explains the status of its implementation along with the next steps to be executed.

1.3 Document Structure

This document is comprised of the following chapters:

Chapter 1 presents an introduction to the project and the document.

Chapter 2 presents the concept that has been developed for using cognitive robotics in remanufacturing tasks and particularly in the demo cases of the R3-Mydas project.

Chapter 3 presents the quality control concept developed for remanufacturing processes, with a particular focus on the laser cladding use case within the R3-Mydas project.

2 Cognitive robotics concept

2.1 Motivation

Modern production lines are designed to maximize the production throughput using machines tailored to perform very specific tasks as fast as possible. When robotics are used, each robotic setup usually repeats the same motion over and over again for its own task, adding a part to an assembly for example. When the production line is reconfigured to produce a different product, the robot program is changed to suit the new product, so the setup time of the production order stays acceptable if the batch size is significant.

However, in remanufacturing tasks, each item being processed necessitates a tailored robotic intervention as even though the task stays constant, the history of the product to remanufactured is different so the processing will be adapted. For example, in a production line remanufacturing gears, the wear on each gear will be assessed and repairs will be made only to the teeth that present signs of wear and/or damage. Therefore, the whole robotic task will change from gear to gear.

This need for adaptability calls for increased intelligence in the robotic system. This intelligence is divided in 3 categories:

1. Perception: the robot needs to perceive the object it has to handle in terms of position, dimensions, defects and other factors. This is usually performed via computer vision
2. Reasoning: the robot needs to infer the task to be achieved on the object depending on what it has perceived. This is usually programmed on the robot
3. Execution: the robot needs to carry out the task it has set. This is usually performed via path planning and operation of the end-effector

The goal of Task 6.1 – Cognitive Robotics is to demonstrate that it is possible to transfer these intelligence skills to a robotic system and therefore that robotic setups can perform complex remanufacturing tasks.

2.2 Goals

As Work Package 6 aims at supporting the project's demo cases, one was selected to be the first objective of remanufacturing automation. Demo Case 2 – EV Batteries was chosen as there was an obvious synergy to be used having AVL, a battery recycling company, and SPIN, a robotic screwdriver manufacturer, as partners in the project.

The goal is to fully automate the process of disassembling an EV battery without human intervention. This process would benefit a lot from automation because EV batteries are large (1-3 meters) and are very secured because of the danger of high voltage inside so they feature lots of screws on the casing (50-100 pieces in most cases). Removing this many screws manually can take up to an hour for an operator and is a very repetitive task.

Additionally, even though operators performing this task are trained, there remains a risk for electrocution when working so close to high-voltage battery modules. Therefore, this task fits perfectly the "3Ds" of tasks for which robotics bring the most value which are Dull, Dirty and Dangerous tasks.

2.3 Concept

As the scope of the tasks has been defined, it is possible to define a concept to solve this problem. The battery will be placed next to a robotic setup that must detect the screws, go to them and unscrew them one by one until the casing of the battery can be removed for inspection. For safety reasons, the prototype that is used for testing is emptied of all the battery modules as CSEM doesn't have a laboratory certified for battery processing.

First, the perception problem needs to be resolved. There is no available standardized screw detection tool available so a computer vision model will be trained by CSEM to detect screws on the battery The model will be trained to be as generalized as possible, meaning it will be able to detect any type of screw on any object to increase the potential for reuse on other tasks.

Secondly, the execution side must be implemented. The robotic arm should be configured to perform efficient and accurate trajectories. The electric screwdriver from Spin is installed on the robotic arm as the end-effector and synchronized to it for simultaneous control of the two devices.

Finally, the reasoning linking perception and execution is programmed. The position of the screws on the images must be related to the position of the camera at time of capture so that the physical-space position of the screws can be inferred from the pixel-space positions in the images.

2.4 Implementation

The implementation of the concept is in progress as of M18 of the project. The work that has been done so far is described below.

2.4.1 Perception

Object detection & segmentation models need large quantities of examples (~50 000) to reach a high-enough accuracy to be used on an industrial setup. These examples consist of pictures of the object of interest in various environments with the segmentation, i.e. the outline, of the object as label. There is no existing dataset of this type of data for screws available online. Additionally, generating manually this kind of dataset is very tedious and long, having to take many pictures of different screws with many backgrounds. A solution to this limitation is to use synthetic data, which in the context of image examples are realistic pictures of the desired scenes created in a rendering software. CSEM has used synthetic data for multiple projects with success.

For this application, Blender was used to generate tens of thousands of scenes featuring screws in randomized orientations, on randomized surfaces with randomized textures with randomized backgrounds and lighting conditions. The mask describing the segmentation of the screw on the image is generated alongside it to serve as label when training the model. The randomization of all factors has been found to be decisive to make the model perform in any conditions. Some examples are shown in Figure 1.

Figure 1: Examples of scenes generated in Blender to train the screw detection model.

These examples are then used to train a HRNet [REF-27] for screw detection and segmentation. It is composed of 1097 layers with a total of 9,636,242 trainable parameters which corresponds to a model size of 36.76 MB, which is quite small and ensures its computational efficiency. The model is tested with the demo case camera on the demo case battery to reproduce the robotic setup's conditions. Initial performance was already quite good with the drawback of detecting screwless holes as false positives. Indeed, holes without screws look very similar to holes with screws especially on reflective surfaces like the battery's metal and with dark screws such as the ones featured on the battery. This problem was removed by generating new examples featuring screwless holes as counterexamples which solved the false positives issue.

On the robotic installation, the battery is very large and therefore it is impossible to take a picture of the whole battery and identify all screws. It is then needed to scan the battery for screws with the camera. The selected camera is attached to the end-effector of the robot with a 3D-printed adaptor and a scanning trajectory is implemented on the robot.

Since the scanning implies taking multiple pictures of each screw, as the model is run on each frame of the video feed given by the camera during scanning, tracking of each screw is implemented too. For each new screw appearing in the field of view, a unique ID is generated for it and on the next frame, if the position of a screw is very close to the position of one in the previous frame, they are associated with the same screw ID. This allows to keep track of the number of screws and more importantly, gathers the multiple points of view of each screw from different angles together which will be essential during screw triangulation later on. An example of model output is shown in Figure 2.

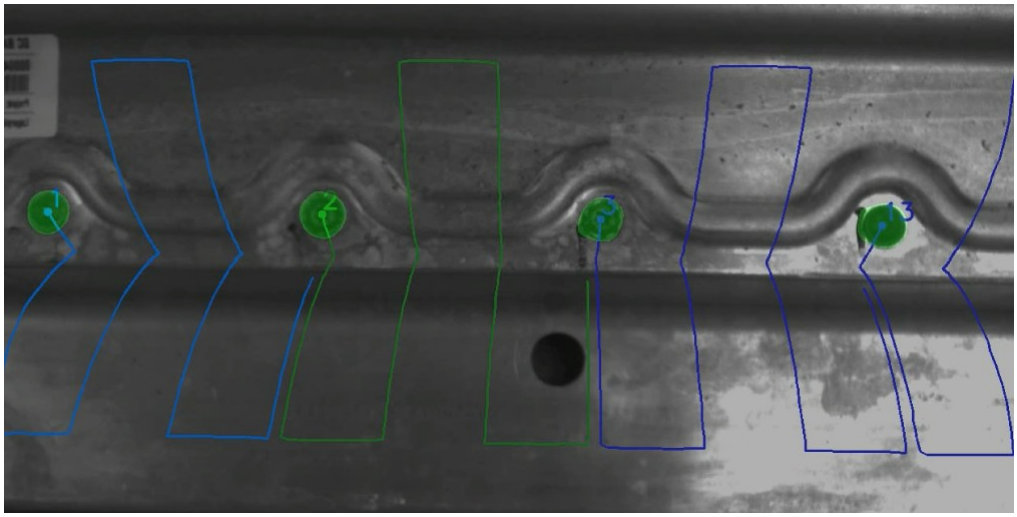

Figure 2: Output of the vision model on the test battery with segmentation (green circles) and tracking (coloured lines).

2.4.2 Reasoning

After scanning of the battery, a dataset containing the pixel-space position of the screw alongside the camera position at capture time for each image for each screw ID is generated. The projection matrix of each point of capture is computed, it encapsulates the coordinate transformation from pixel-space position in the image to physical-space position on the battery. The projection matrices and pixel-space detected screw positions are then used in a triangulation algorithm that finds the point in the physical space where the screw is most likely to be depending on the information contained by all the images where that specific screw appeared. An illustration of this algorithm is shown in Figure 3.

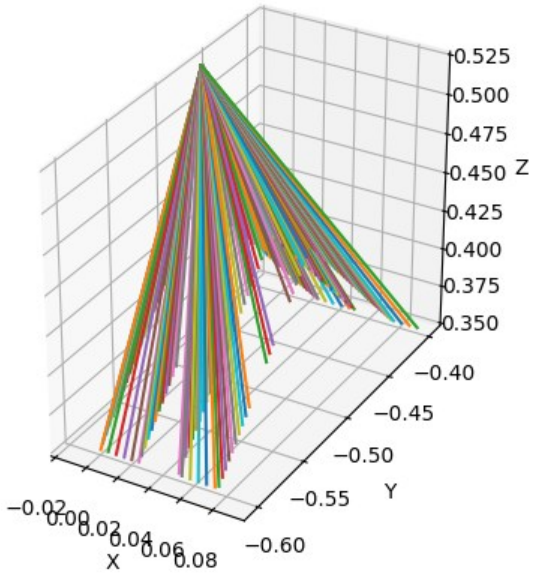

Figure 3: Illustration of the triangulation rays from each camera capture point to the predicted position of the screw.

This process is repeated for all screw IDs until a position prediction is obtained for each screw ID. This is represented in Figure 4.

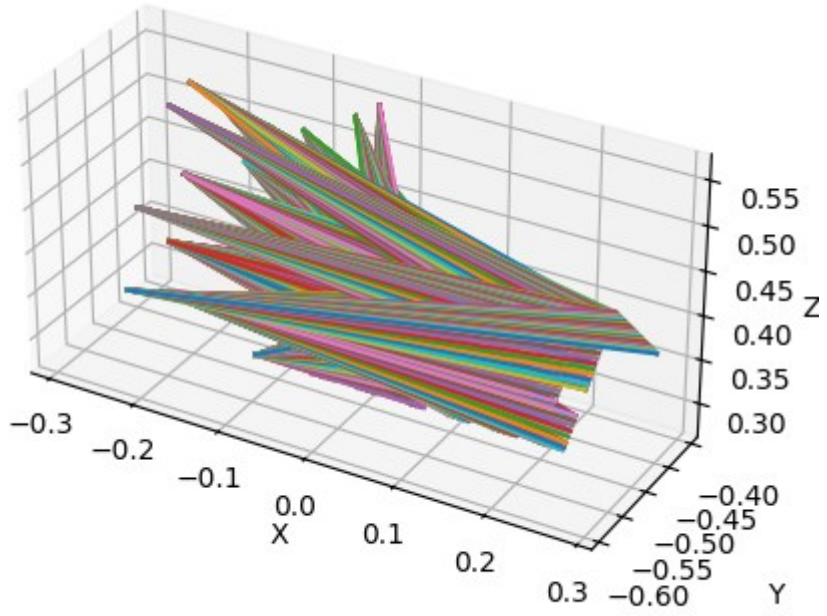

Figure 4: Illustration of the triangulation rays for all screws.

2.4.3 Execution

Once the screw positions in physical space have been computed, the disassembly task can be executed.

Because SPIN's electrical screwdriver is tailored for applications where positions are taught once by using the collaborative feature of the robot and repeated identically over time, it cannot be used out of the box for this application that necessitates more flexibility. The main script running the disassembly process needs to be able to control each aspect of the unscrewing process. This is why the backend functions of the screwdriver are accessed in Python instead of using the User Interface provided with SPIN's products.

The robot is programmed to perform the following:

- Move towards a screw position and approach it from the top
- Gently go down until the force sensor detects resistance indicating contact with the screw head
- Start the unscrewing process and continue it until the sensed torque decreases below a threshold indicating that the screw is loosened
- Move up slightly
- Repeat this process for each screw position

This process is illustrated in Figure 5 where 3 screws are already loosened on the bottom left and one is currently being unscrewed.

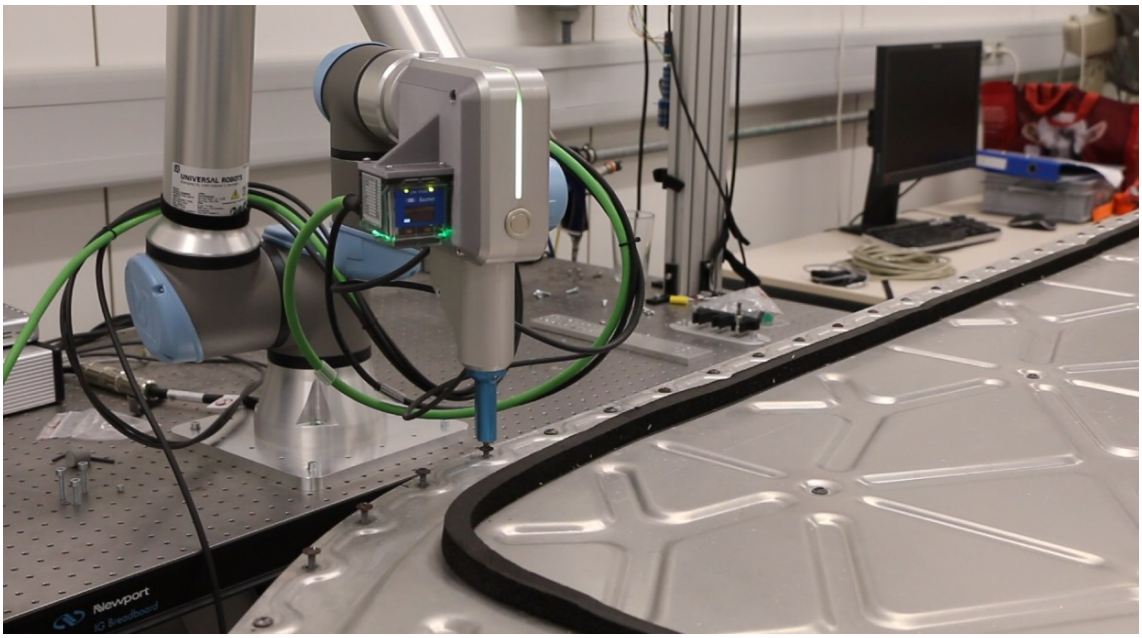

Figure 5: Photo of the electric screwdriver mounted on the robot arm in the process of removing screws from the test battery.

2.5 Next steps

The process described above is functional but can be prone to slight position errors due to the triangulation algorithm or calibration of the camera that can add up to a few millimetres. However, the unscrewing task calls for up to millimetre accuracy. Indeed, the electric screwdriver has to land almost exactly in the center of the screw head to remove it properly. Because of this limitation, it was planned to carry out the task in 2 parts:

- First guess of screw position from the method described above
- Refinement of screw position as it is approached with motion maps

The idea for the second part is to control the robot to move towards the screw position while computing a new more accurate guess on the screw position at each time step as illustrated in Figure 6.

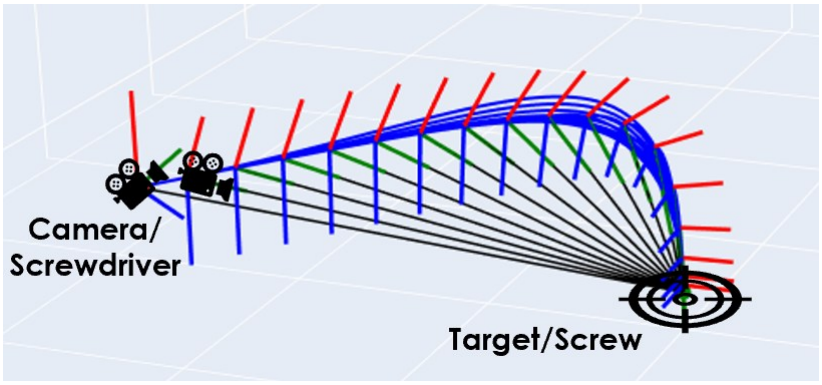

Figure 6: Illustration of screw position refinement while in motion.

To do that, one method is to use motion maps. In this method, synthetic data is also used. It consists of generating thousands of randomized scenes with screws as described before with randomized camera positions and generate a robot command for each example that would get the camera closer to the objective object. This command can simply be the difference in position and orientation between the camera and the object multiplied by a factor to choose the size of the step taken at each iteration. This robot command is then encoded onto images describing the cartesian motion (X, Y, Z) and rotation (Rx, Ry, Rz) as illustrated in Figure 7.

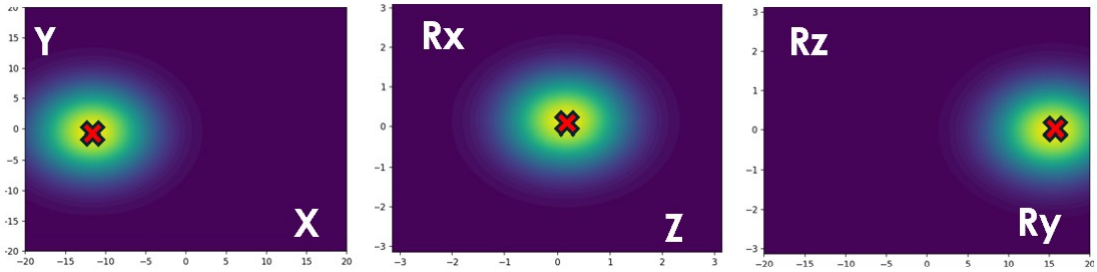

Figure 7: Illustration of the motion maps generation.

This set of images is then combined together in one single image, taking advantage of the 3 channels offered by the RGB image format, producing the output shown in Figure 8.

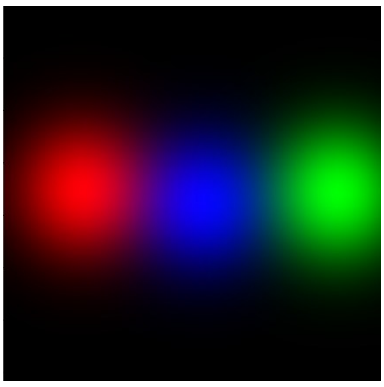

Figure 8: Final motion map output example.

By generating motion map examples for thousands of scenes, the model is trained to encode in the motion map the relevant robot command to approach the screw from any direction. At execution time, feeding the frame from the camera in real time to the model will produce a motion map that can be decoded into actual robot motion, which is in turn sent to the robot arm. This is repeated at each time step and produces a trajectory that will converge to the screw head to perform disassembly.

This will be implemented by CSEM in the coming months.

3 Quality control concept

3.1 Motivation

In conventional manufacturing environments, quality control processes are typically optimized for consistency and repetition. Inspections are often rule-based and designed around uniform products and predictable process outcomes, allowing pre-defined thresholds to accept or reject produced parts. In contrast, in remanufacturing contexts, such as the laser cladding of crankshafts and gears, every part in the process has a different geometry, wear pattern, and repair requirements due to its usage history. While the cladding task for restoring worn crankshafts and bearing surfaces remains functionally similar, the thermal behaviour, scan path, and material response can vary from one crankshaft to another [REF-22].

As a result, standardized quality control routines are insufficient to guarantee consistent part quality in remanufacturing. Instead, there is a need for a more adaptive and data-driven quality control strategy. Ideally, it can evaluate each process instance individually based on predicted or measured key control characteristics, such as thermal profiles, and account for local geometry and process conditions. This motivates the development of fast, flexible, and generalizable modelling approaches. In this context neural operator-based surrogate models show a promising potential: they enable rapid, geometry-aware prediction of temperature fields from varying process parameters and initial conditions.

These surrogates function as real-time predictive modules within a closed-loop control system, continuously evaluating the thermal response of the laser cladding process. By enabling close to real-time inference of temperature fields, the model provides immediate feedback to the control logic, allowing dynamic adjustment of process parameters. This real-time responsiveness is critical for remanufacturing applications, where batch sizes are small and the variability between components is high.

3.2 Goals

The goal of this work is to implement an adaptive, data-driven quality control framework for laser cladding in crankshaft remanufacturing, based on neural operator models. These models are intended to act as fast, accurate and generalizable surrogates for the thermal modelling of the laser cladding process, capable of supporting variable process conditions. The objectives involve the following:

- Develop fast and generalizable neural operator surrogate capable of predicting the thermal evolution during laser cladding. The model should be efficient enough for use in near real-time monitoring or control.
- Implement predictive evaluation layer that extracts quality indicators, such as peak temperature, thermal gradients and cooling rates. These metrics are

approximations for physical quality features, including hardness, and residual stresses.

- Preliminary work for an eventual integration with an in-situ monitoring systems or closed-loop control framework, where the surrogate model could serve as a digital instance of the physical component.

3.3 State of the Art

Metal additive manufacturing, especially Directed Energy Deposition (DED) using powder feedstock, faces persistent challenges related to process inefficiencies and variability in product quality [REF-03, REF-06]. These challenges are due to complex transient thermal and mechanical phenomena that govern melt pool dynamics, microstructure evolution, residual stresses, and the formation of defects.

High-fidelity physics-based simulations can accurately capture these phenomena by solving coupled partial differential equations (PDEs) describing heat transfer, fluid flow, and mechanical deformation [REF-04]. Despite their accuracy, their significant computational cost limits their applicability to real-time process control [REF-02]. As a result, data-driven approaches utilizing machine learning (ML) have gained popularity as a promising alternative to predict key process outcomes such as thermal fields, residual stress distributions, and defect formation [REF-07, REF-21, REF-26]. Recent advancements, such as Recurrent Neural Networks (RNNs) [REF-20] and Long Short-Term Memory (LSTM) [REF-11] models have shown an improved ability to capture spatiotemporal dependencies, even for long-term simulations. Graph Neural Networks (GNNs) [REF-18] further enhance this by providing a flexible, geometry-agnostic representation of complex unstructured geometries, to predict thermal responses. Similarly, Physics-Informed Neural Networks (PINNs) have also been applied to modelling different phenomena in additive manufacturing by embedding governing physical laws directly into the training process. This allows PINNs to achieve accurate predictions even with limited labelled data [REF-09, REF-14]. However, despite their interpretability and data efficiency, PINNs often face scalability issues and high training costs when applied to large or highly dynamic systems [REF-08]. A different approach for data-driven modelling in metal additive manufacturing are Neural Ordinary Differential Equations (NODEs), which present a different way to predict transient dynamics, such as residual stress evolution [REF-10]. By learning the underlying system dynamics through neural networks and continuous transformations, NODEs can outperform traditional RNNs in dynamic prediction tasks.

To overcome the limitations of traditional machine learning models based on feed forward neural networks, recent research has increasingly focused on neural operator (NO) architectures [REF-17]. Unlike point wise function approximators such as RNNs and LSTMs, which often exhibit limited generalizability across varying process parameters and depend on fixed mesh discretizations, neural operators are designed to learn the

nonlinear operators that govern the underlying partial differential equations (PDEs) of physical systems. This approach is based on the universal approximation theorem for nonlinear operators, introduced by Chen and Chen [REF-23], which proves that neural networks can approximate any continuous nonlinear functional or operator given sufficient capacity.

The Deep Operator Network (DeepONet) was the first neural operator architecture proposed and has shown promising results in modelling multiphysics phenomena relevant to additive manufacturing. In [REF-13] a parametric DeepONet architecture was trained on high-fidelity multiphysics simulation data to predict sequentially coupled thermo-mechanical field data from a simplified DED process.

Building on this foundation, Fourier Neural Operators (FNOs) have emerged as one of the most widely used and effective neural operator architectures. By leveraging the Fast Fourier Transformation in their architecture, FNOs enable efficient, mesh-independent learning of PDE solution operators [REF-15]. Both Liu et al. [REF-16] and Chen et al. [REF-05] demonstrate the capability of FNOs to predict thermal fields for metal additive manufacturing. Liu et al. [REF-16] integrate FNOs into a digital twin framework for Laser Powder Bed Fusion (L-PBF), enabling real-time prediction of melt pool temperature fields and defect indicators from process parameters, supporting closed-loop control. However, in this approach only the steady-state temperature field for given process parameters is predicted, without accounting for the dynamic effects of the scan path, temporal evolution, or part-scale temperatures. In contrast, Chen et al. [REF-05] applied FNOs to Directed Energy Deposition (DED), focusing on localized heat-affected zones using a window-based model that enables part-scale temperature prediction over time and generalization to new geometries, yet the approach remains constrained by low spatial resolution and does not generalize to previously unseen process parameters.

Recent developments in neural operator research have introduced architectures that improve scalability, generalization across geometries, and the ability to model complex, multi-scale physical systems as in metal additive manufacturing. [REF-01], introduce a latent-space modelling paradigm that flexibly encodes grid- and particle-based simulations into a compact latent representation. This enables efficient time evolution and querying at arbitrary spatio-temporal points. Similarly, the Transolver architecture [REF-25] introduces a novel physics-attention mechanism for learning solution operators on unstructured meshes achieving efficient operator learning on industrial-scale problems. In Wen et al. [REF-24] the authors address the challenge of learning PDE solution operators on arbitrary domains by combining multiscale attention graph encoders, geometry embeddings, and transformer-based latent processing. These architectures have shown to overcome the caveats of models like FNOs and DeepONets, offering solutions for building large-scale surrogate models for complex processes.

In summary, while significant progress has been made in data-driven surrogate modelling in metal additive manufacturing, current approaches still face limitations in

terms of spatial resolution, temporal dynamics, geometric generalization, and adaptability to varying process parameters. Hence, neural operator architectures and geometry-aware models can address these challenges, yet their application to real-time, high-fidelity modelling of AM processes remains a challenge.

3.4 Concept

The main focus of the concept presented evolves around the neural operator surrogate model, which ideally replaces slow high-fidelity simulations with a data-driven model able to predict the thermal field evolution during the laser cladding process. The surrogate model enables near real-time prediction of the temperature distribution, given a set of input conditions: the initial temperature, scan trajectory, and process parameters such as the laser power.

By combining this surrogate with a quality monitoring and control loop, the system is able to infer quality outcomes driven by the temperature evolution. This becomes important in remanufacturing contexts, where each part has a different wear pattern and process conditions may vary from part to part.

3.4.1 Predictive Surrogate Model

The neural operator model is used to predict the evolution of the thermal field close to real-time. It takes the current process setup, such as the initial conditions, scan path and process parameters, as input and returns a prediction of the temperature field over time. The operator architecture enables generalization across different scan paths and a range of different process parameter.

Two architectures were explored:

- Fourier Neural Operators (FNOs) [REF-15]: The architecture leverages the Fast Fourier Transform to learn physical dynamics in spectral space
- Convolutional Neural Operators (CNOs) [REF-19]: CNOs use resolution-independent convolution kernels to capture multi-scale features of the underlying process in a spatially localized manner.

3.4.2 Quality Indicator Extraction

From the predicted thermal field, critical indicators are computed to support the decision making and control:

- Peak temperature – risk of overheating or melting anomalies
- Thermal gradients – associated with residual stress development and cracking potential
- Cooling rates – correlate with the resulting hardness

These indicators can be derived from the surrogate's predictions and serve as predicted approximations for physical quality metrics. Especially, the resulting hardness which

correlates with the cooling rates is a key feature for the remanufacturing of wear resistant crankshafts.

3.4.3 Decision and Feedback

The extracted indicators are compared against predefined quality thresholds or tolerances, which are determined in discussions with the project partners. If one or more metrics exceed the specified limits, the parameter set, such as the laser power or scan path, can be marked for revision. The fast inference of the model allows this evaluation to be performed iteratively within a pre-process planning stage or eventually in a closed-loop control system.

Eventually, the model could be used in an advanced setting within a real-time control loop, continuously predicting the thermal response during the printing process. This would enable dynamic adjustment of parameters (e.g. laser power) to maintain thermal conditions within acceptable ranges during the process.

3.5 Implementation

3.5.1 Data Generation and Preprocessing

Training data is generated using the Add2Man software developed by CIMNE (Barcelona). It is an experimentally validated, high-performance code developed for the simulation of additive manufacturing processes such as laser cladding, L-PBF, and friction stir welding. The use of this software allows for direct control of the process settings and numerical properties. As a first step, the focus is put on 2D thermal simulations under various scan and parameter configurations. A data pipeline extracts structured datasets from these simulations, which are used to train the data-driven model. This procedure involves the following: read-in temporal sequences and spatial meshes from simulation, normalize and encode simulation data and extract the structured input-output pairs.

3.5.2 Surrogate Model Development

Autoregressive Temporal Modelling

An autoregressive prediction and training strategy is implemented to model the evolution of the thermal field over time. This means the model predicts the temperature field at the next time step based on the current field and the process parameters. This approach allows the model to generalize across variable rollout lengths and be usable in a sequential prediction setup, where predictions are updated as new process data becomes available.

To improve training stability and reduce memory usage, temporal bundling is applied. Instead of predicting a single future step at each iteration, the model predicts a bundle of consecutive timesteps in a single forward pass. This reduces the number of recursive steps, improves training efficiency and long-term accuracy.

Performance of the Models

After training, the model is evaluated on a test set consisting of unseen scan paths and process parameter settings to assess the performance and accuracy. To quantify the accuracy of the predictions three metrics were used: L1 error, L2 error, and R2 score. The L1 and L2 error quantify the absolute deviation in predicted versus true temperature fields, while the R2 score measures the variance of the prediction across the domain, with a value of 1.0 indicating perfect predictions.

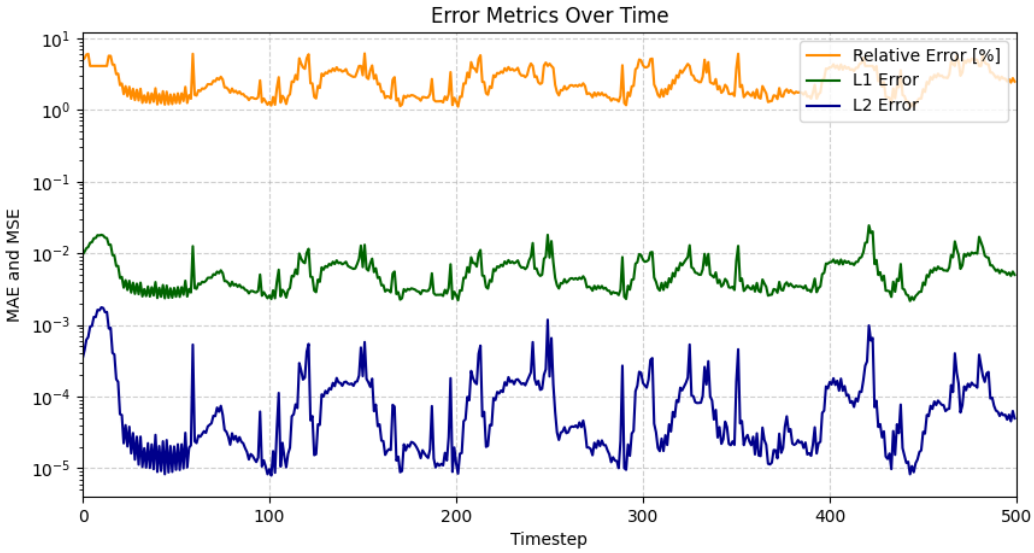

Figure 9: Error metrics (relative error, L1 and L2) for the predictions for each timestep. Here the trained FNO model is evaluated on an unseen test trajectory. The maximum relative error is at 6.12 %, while the maximum L1 error is 0.024 and the maximum L2 error at 0.002.

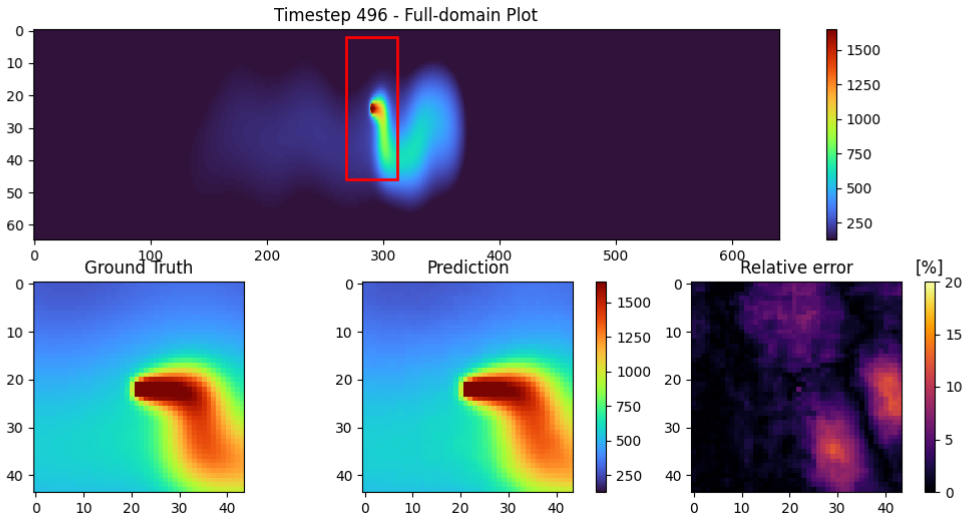

Figure 10: Prediction of the trained model after 496 timesteps. The model is based on the FNO architecture. As input for the prediction the model has only seen the initial temperature at timestep 0 and the current process setup (parameter and scan path).

Early results in the 2D setting show that the models' predictions are accurate and stable over whole trajectories. Both tested architectures achieved L2 errors consistently below 0.01 and R2 scores of up to 0.97 for the whole scan sequence. Additionally, as seen in Figure there is no significant drift in the autoregressive rollout that would indicate an error accumulation. Figure shows the temperature prediction of the trained FNO model for timestep 496. The prediction of the temperature evolution is only based on the initial temperature field for timestep 0 and the laser power and movement at each timestep.

3.6 Extensions and Next steps

Building on the current 2D modelling results, the following extensions and future tasks are planned:

- Transition from 2D to 3D modelling of the laser cladding process and therefore improve spatial fidelity and predictive robustness for real-world applications.
- Integration with measurement data to compare the predicted and actual thermal fields. If applicable, extension online comparison of model predictions and empirical measurements.
- Expand towards real-time predictive control applications, by coupling the surrogate with a closed-loop control system or model predictive control framework.

4 References

[REF-01]	Alkin, B., Fürst, A., Schmid, S., Gruber, L., Holzleitner, M., Brandstetter, J., 2025. Universal Physics Transformers: A Framework For Efficiently Scaling Neural Operators. https://doi.org/10.48550/arXiv.2402.12365
[REF-02]	Bartlett, J.L., Li, X., 2019. An overview of residual stresses in metal powder bed fusion. Additive Manufacturing 27, 131–149. https://doi.org/10.1016/j.addma.2019.02.020
[REF-03]	Bastola, N., Jahan, M.P., Rangasamy, N., Rakurty, C.S., 2023. A Review of the Residual Stress Generation in Metal Additive Manufacturing: Analysis of Cause, Measurement, Effects, and Prevention. Micromachines 14, 1480. https://doi.org/10.3390/mi14071480
[REF-04]	Bayat, M., Dong, W., Thorborg, J., To, A.C., Hattel, J.H., 2021. A review of multi-scale and multi-physics simulations of metal additive manufacturing processes with focus on modeling strategies. Additive Manufacturing 47, 102278. https://doi.org/10.1016/j.addma.2021.102278
[REF-05]	Chen, J., Xu, W., Baldwin, M., Nijhuis, B., den Boogaard, T. van, Grande Gutiérrez, N., Prabha Narra, S., McComb, C., 2024. Capturing Local Temperature Evolution During Additive Manufacturing Through Fourier Neural Operators. Journal of Manufacturing Science and Engineering 146. https://doi.org/10.1115/1.4065316
[REF-06]	Chen, S., Gao, H., Zhang, Y., Wu, Q., Gao, Z., Zhou, X., 2022. Review on residual stresses in metal additive manufacturing: formation mechanisms, parameter dependencies, prediction and control approaches. Journal of Materials Research and Technology 17, 2950–2974. https://doi.org/10.1016/j.jmrt.2022.02.054
[REF-07]	Era, I.Z., Farahani, M.A., Wuest, T., Liu, Z., 2023. Machine learning in Directed Energy Deposition (DED) additive manufacturing: A state-of-the-art review. Manufacturing Letters, 51st SME North American Manufacturing Research Conference (NAMRC 51) 35, 689–700. https://doi.org/10.1016/j.mfglet.2023.08.079
[REF-08]	Fernández De La Mata, F., Gijón, A., Molina-Solana, M., Gómez-Romero, J., 2023. Physics-informed neural networks for data-driven simulation: Advantages, limitations, and opportunities. Physica A: Statistical Mechanics and its Applications 610, 128415. https://doi.org/10.1016/j.physa.2022.128415
[REF-09]	Hosseini, E., Scheel, P., Müller, O., Molinaro, R., Mishra, S., 2023. Single-track thermal analysis of laser powder bed fusion process: Parametric solution through physics-informed neural networks. Computer Methods in Applied Mechanics and Engineering 410, 116019. https://doi.org/10.1016/j.cma.2023.116019

[REF-10]	Kannapinn, M., Roth, F., Weeger, O., 2024. Digital twin inference from multi-physical simulation data of DED additive manufacturing processes with neural ODEs. https://doi.org/10.48550/arXiv.2412.03295
[REF-11]	Karkaria, V., Goeckner, A., Zha, R., Chen, J., Zhang, J., Zhu, Q., Cao, J., Gao, R.X., Chen, W., 2024. Towards a digital twin framework in additive manufacturing: Machine learning and bayesian optimization for time series process optimization. Journal of Manufacturing Systems 75, 322–332. https://doi.org/10.1016/j.jmsy.2024.04.023
[REF-12]	Kushwaha, S., Park, J., Koric, S., He, J., Jasiuk, I., Abueidda, D., 2024. Advanced deep operator networks to predict multiphysics solution fields in materials processing and additive manufacturing. Additive Manufacturing 88, 104266. https://doi.org/10.1016/j.addma.2024.104266
[REF-13]	Kushwaha, S., Park, J., Koric, S., He, J., Jasiuk, I., Abueidda, D., 2024. Advanced deep operator networks to predict multiphysics solution fields in materials processing and additive manufacturing. Additive Manufacturing 88, 104266. https://doi.org/10.1016/j.addma.2024.104266
[REF-14]	Li, S., Wang, G., Di, Y., Wang, L., Wang, H., Zhou, Q., 2023. A physics-informed neural network framework to predict 3D temperature field without labeled data in process of laser metal deposition. Engineering Applications of Artificial Intelligence 120, 105908. https://doi.org/10.1016/j.engappai.2023.105908
[REF-15]	Li, Z., Kovachki, N., Azizzadenesheli, K., Liu, B., Bhattacharya, K., Stuart, A., Anandkumar, A., 2021. Fourier Neural Operator for Parametric Partial Differential Equations.
[REF-16]	Liu, N., Li, X., Rajanna, M.R., Reutzel, E.W., Sawyer, B., Rao, P., Lua, J., Phan, N., Yu, Y., 2024. Deep Neural Operator Enabled Digital Twin Modeling for Additive Manufacturing.
[REF-17]	Liu, S., Yu, Y., Zhang, T., Liu, H., Liu, X., Meng, D., 2025. Architectures, variants, and performance of neural operators: A comparative review. Neurocomputing 130518. https://doi.org/10.1016/j.neucom.2025.130518
[REF-18]	Mozaffar, M., Liao, S., Lin, H., Ehmann, K., Cao, J., 2021. Geometry-agnostic data-driven thermal modeling of additive manufacturing processes using graph neural networks. Additive Manufacturing 48, 102449. https://doi.org/10.1016/j.addma.2021.102449
[REF-19]	Raonić, B., Molinaro, R., De Ryck, T., Rohner, T., Bartolucci, F., Alaifari, R., Mishra, S., de Bézenac, E., 2023. Convolutional Neural Operators for robust and accurate learning of PDEs
[REF-20]	Ren, K., Chew, Y., Zhang, Y.F., Fuh, J.Y.H., Bi, G.J., 2020. Thermal field prediction for laser scanning paths in laser aided additive manufacturing

	by physics-based machine learning. Computer Methods in Applied Mechanics and Engineering 362, 112734. https://doi.org/10.1016/j.cma.2019.112734
[REF-21]	Saimon, A.I., Yangue, E., Yue, X., Kong, Z.J., Liu, C., 2024. Advancing Additive Manufacturing through Deep Learning: A Comprehensive Review of Current Progress and Future Challenges.
[REF-22]	Sousa, S.D., Pham, D.T., 2023. Quality Control in Remanufacturing: Distinguishing Features and Techniques, in: Kim, K.-Y., Monplaisir, L., Rickli, J. (Eds.), Flexible Automation and Intelligent Manufacturing: The Human-Data-Technology Nexus. Springer International Publishing, Cham, pp. 546–555. https://doi.org/10.1007/978-3-031-17629-6_57
[REF-23]	Tianping Chen, Hong Chen, 1995. Universal approximation to nonlinear operators by neural networks with arbitrary activation functions and its application to dynamical systems. IEEE Trans. Neural Netw. 6, 911–917. https://doi.org/10.1109/72.392253
[REF-24]	Wen, S., Kumbhat, A., Lingsch, L., Mousavi, S., Zhao, Y., Chandrashekar, P., Mishra, S., 2025. Geometry Aware Operator Transformer as an Efficient and Accurate Neural Surrogate for PDEs on Arbitrary Domains. https://doi.org/10.48550/arXiv.2505.18781
[REF-25]	Wu, H., Luo, H., Wang, H., Wang, J., Long, M., 2024. Transolver: A Fast Transformer Solver for PDEs on General Geometries. https://doi.org/10.48550/arXiv.2402.02366
[REF-26]	Xiao, S., Li, J., Wang, Z., Chen, Y., Tofighi, S., 2024. Advancing Additive Manufacturing Through Machine Learning Techniques: A State-of-the-Art Review. Future Internet 16, 419. https://doi.org/10.3390/fi16110419
[REF-27]	Wang, Jingdong, et al. "Deep high-resolution representation learning for visual recognition." *IEEE transactions on pattern analysis and machine intelligence* 43.10 (2020): 3349-3364.